Int. J. Electrochem. Sci., 14 **(2019)** 2893 – 2905, doi: 10.20964/2019.03.29

International Journal of ELECTROCHEMICAL SCIENCE
www.electrochemsci.org

Photoelectrochemical Degradation of 4-Nitrophenol using CuO-ZnO/exfoliated graphite Nanocomposite Electrode

Onoyivwe Monday Ama[1,3,*], *Khotso Khoele*[2,3], *William Wilson Anku*[1], *Suprakas Sinha Ray*[1,3]

[1] Department of Applied Chemistry, University of Johannesburg, Doornfontein, 2028 South Africa.
[2] Tshwane University of Technology, Department of Chemical, Metallurgical and Materials Engineering, Pretoria, South-Africa
[3] DST/CSIR National Center for Nano-structured Materials, Council for Scientific and Industrial Research, Pretoria 0001 South Africa.
[*]E-mail: onoyivwe4real@gmail.com

Received: 25 October 2018 / *Accepted:* 3 December 2018 / *Published:* 7 February 2019

There has been a focused attention on the degradation of phenol and its nitro derivatives in industrial wastewater prior to its discharge into the environment due to the carcinogenic potential of these pollutants on biota. Hence, this study focused on the application of photoelectrochemical technique in the degradation of 4-Nitrophenol from simulated wastewater by using synergistic photoactive material (CuO-ZnO) combined with exfoliated graphite (EG) through co-precipitation method. The experiment was performed using EG, CuO-ZnO and EG/CuO-ZnO electrodes. Characterization techniques engaged to assess the morphology, crystallinity, surface area and chemical properties of the composites include SEM, TEM, XRD, UV-Vis and FTIR spectroscopies. The XRD analysis revealed that the CuO and ZnO exist in cubic and hexagonal phases respectively. SEM analysis showed a good dispersion of the CuO-ZnO onto the EG. The modification of the CuO-ZnO with EG endowed the composite with a larger surface area and strong light absorption in the visible light region. All the fabricated electrodes degraded the dye. However, the EG/CuO-ZnO demonstrated the highest degradation efficiency. The EG showed the least efficiency. The EG/CuO-ZnO was also used in the degradation of the dye on the basis of three techniques namely photolysis, electrochemical, and photoelectrochemical methods. The photoelectrochemical method showed a faster degradation when compared with photolysis and electrochemical oxidation. The synergistic effects of CuO, ZnO and EG promoted the efficiency of the EG/CuO-ZnO against the degradation of the dye.

Keywords: Exfoliated graphite, CuO, ZnO, 4-Nitrophenol, photoelectrochemical degradation, photocatalysis.

1. INTRODUCTION

The presence of persistent organic pollutants such as phenol and its nitro derivatives in industrial wastewaters has aroused serious concerns over the past half-century due to the fact that these

chemicals are listed among the leading cancer-causing contaminants [1]. Bio-refractory nitrophenols are released into the environment through untreated wastewater from dyes, petrochemicals, paints, pesticides, pharmaceuticals and wood preservative industries and there is no evidence of their formation from any natural source [2, 3]. Ingestion of nitrophenols and their accumulation in the human body has been reported to cause blood disorder by decreasing the body's ability to carry oxygen to tissues and organs [4]. Prolonged exposure to these substances could also cause eyes and skin irritations [5].

Aiming at reducing nitrophenol pollution from industrial effluents, several techniques have been developed and these include physical adsorption, chemical as well as biological degradation processes. However, most of the reported techniques are either inefficient or give rise to hazardous by-products, resulting in secondary pollution [6]. Considerable attention has been given to decomposition techniques such as advanced oxidation processes (AOPs) which provide a powerful oxidative environment for effective pollutants degradation. Photoelectrochemical degradation process, a combination of heterogeneous photocatalysis and electrochemical oxidation methods, has been used extensively for soluble and stable organic pollutants remediation from wastewater with successful results. The effectiveness of this technology is attributed to the *in situ* generation of highly reactive hydroxyl ($^{\bullet}OH$) and superoxide ($^{\bullet}O_2^-$) radicals by photoactive and conducting materials [7-9]. The produced radicals have the potential to mineralize organic pollutants to water and carbon dioxide. CuO-ZnO nanocomposite is well reported for its application in water treatment [10, 11]. This material has been found to exhibit catalytic activity through degradation under visible-light irradiation due to the irreversible charge transfer from ZnO to CuO, at the p-CuO and n-ZnO band edges [11, 12].

Exfoliated graphite (EG) is an interesting material with outstanding properties which counteract the limitations of most photoactive materials. These properties including high surface area and thermal stability, corrosion resistance and low density [13, 14]. EG has the ability to act as an electron sink that captures and shuttles electrons, thereby diminishing recombination of holes and electrons if fused into a semiconductor for application in photocatalysis [1]. Therefore, EG can serve as a model of porous carrier substrate for superior photoelectrochemical degradation process. Hence, the current work reports the fabrication and application of EG/ZnO−CuO electrode for the degradation of stable and soluble 4-Nitrophenol in aqueous phase using a photo-assisted electrochemical technique.

2. EXPERIMENTAL SECTION

2.1 Materials and Characterisations

Materials used were graphite flakes, copper (II) oxide, zinc oxide, sulphuric acid, nitric acid, polyethylene glycol, ammonia, Zinc acetate dehydrate (≥98%), copper acetate (98%), 4-Nitrophenol (≥99%). All chemical were used as received from the suppliers without further purification. Deionized water (DI) was used for solution preparation.

2.2 Synthesis of EG

Natural graphite (20g) was poured into H_2SO_4: HNO_3 (3:1v/v) mixture and the mixture was left for 24 h. Thereafter, the mixture was washed several times with deionized water until the pH reached 7. The obtained graphite intercalated compound (GIC) was dried in an oven (100° C) for 12 h. Furthermore, the GIC was subjected to thermal treatment in an electric furnace at 800° C for 1 min. This procedure resulted in the puffed material called EG.

2.3 Preparation of CuO-ZnO Nanocomposite

The CuO-ZnO nanocomposite was synthesised using the co-precipitation method. Firstly, equimolar masses of zinc acetate dihydrate and copper acetate were dissolved in 100 mL of distilled water. After dissolution, sodium carbonate (2X molar of copper acetate) was added to the above mixture and the solution was stirred at 85 °C for 6 h. The obtained precipitate was collected by centrifugation using water (three times) and ethanol respectively. The precipitate was dried in an air oven at 80 °C for 12 h. Later on, the sample was calcined in an alumina crucible at 450 °C for 3 h using a muffle furnace.

2.4 Fabrication of the EG Electrode

For the fabrication of the electrodes, Cu wire, glass rod, and conducting silver paint were used. Herein, Cu wire was coiled at the edge, and it was covered with epoxy resin. 1 cm diameter pellet of EG (150 mg) was compressed and placed at the surface of the coiled Cu wire using a tube glass to prevent it from touching the solution.

2.5 Preparation of EG/CuO-ZnO Electrode

EG was poured into deionized water in a ratio of 1:1. The combination was constantly stirred for 12 h and afterwards sonicated for 6 h. The CuO-ZnO (1g) obtained from Section 2.3 was then added to the dispersed EG and the mixture was sonicated for another 4 h. Subsequently, the mixture was dried in an oven for 6 h at 100 ℃. The EG/CuO-ZnO nanocomposite was compacted to produce a pellet which was then used for the fabrication of electrode.

2.6 Degradation Experiment

All the degradation experiments were performed under galvanostatic control at the voltage range between 2V-5V and a corresponding current range of 1mA-15mA. A solar simulator fitted with a UV filter was used to provide the visible light for the experiment. Within the setup to study the degradation and the kinetics of the 4-Nitrophenol, the distance between the New Port 9600 Full Spectrum solar simulator equipped with 400 W and the experimental setup was measured to be 10 cm.

The beam power was equivalent to 1 sun. The prepared 4-Nitrophenol solutions (100 mL, 20 mg/L) were transferred into the electrochemical cell, and 0.1 M sodium sulphate was added to the solution to enhance its conductivity. The electrodes were then connected to the electrochemical instrument. The EG/CuO-ZnO was used as a working electrode, while Ag/AgCl (3.0 M KCl) and platinum foil were used as reference and counter electrodes, respectively. The system was switched on and the degradation experiment was performed. 5 mL aliquots of the degraded samples were taken from the electrochemical cell at different time intervals (50, 100, 150, 200, 250, 300 min) using a disposable syringe and filtered through 0.4 μm PVDF membrane filter. Shimadzu UV-2450 was then used to determine the extent of the degradations of the supernatant solutions.

The photoelectrochemical degradation was carried out using the electrodes under visible light illumination. The electrochemical degradation was executed with the electrode only (in the absence of visible light), while the photolysis procedure was performed with visible light only, i.e., no electrode was employed.

2.7 Characterization Techniques

The surface profiles of nanocomposites used to degrade 4-Nitrophenol were carried out using scanning electron microscopy (SEM) coupled with energy-dispersive X-ray spectroscopy (EDS). The EDS inclusion was particularly for elemental analysis on each sample. To examine the crystalline structures and phases present in each photoanode used in this study, X-ray diffraction (XRD) was applied. The XRD instrument used was Philips PAN analytical X'Pert, and the operational settings were set at 40 kV of voltage, Cu Kα radiation of $\lambda = 0.15418$ nm and 2θ step size. Furthermore, surface area, pore size, and pore volume information were acquired through the use of micromeritics Trista II surface area and porosity analyzer. Lambda 750S UV/VIS Spectrometer was used to determine the optical activities of the nanocomposites and the extent of the degradations of the pollutant.

3. RESULTS AND DISCUSSION

3.1 SEM and EDX analyses

Fig. 1 shows the SEM morphologies of the nanocomposites synthesized in this work. EG morphology is shown in Fig. 1a, and it is identified to have layered structures of varied sizes. In Fig. 1b, the CuO-ZnO nanocomposite shows small and spherical shapes with clear boundaries. On the other hand, the mixed nanocomposite (EG/CuO-ZnO) morphology is shown in Fig. 1c. It can be seen that the CuO-ZnO composites spread uniformly on the surface of the EG. EDX analysis, which is shown in Fig. 1d, shows Zn, Cu, O and C as elemental components of the EG/CuO-ZnO nanocomposite. The co-presence of these elements in the fabricated sample indicates a successful fabrication of the intended EG/CuO-ZnO [15, 16].

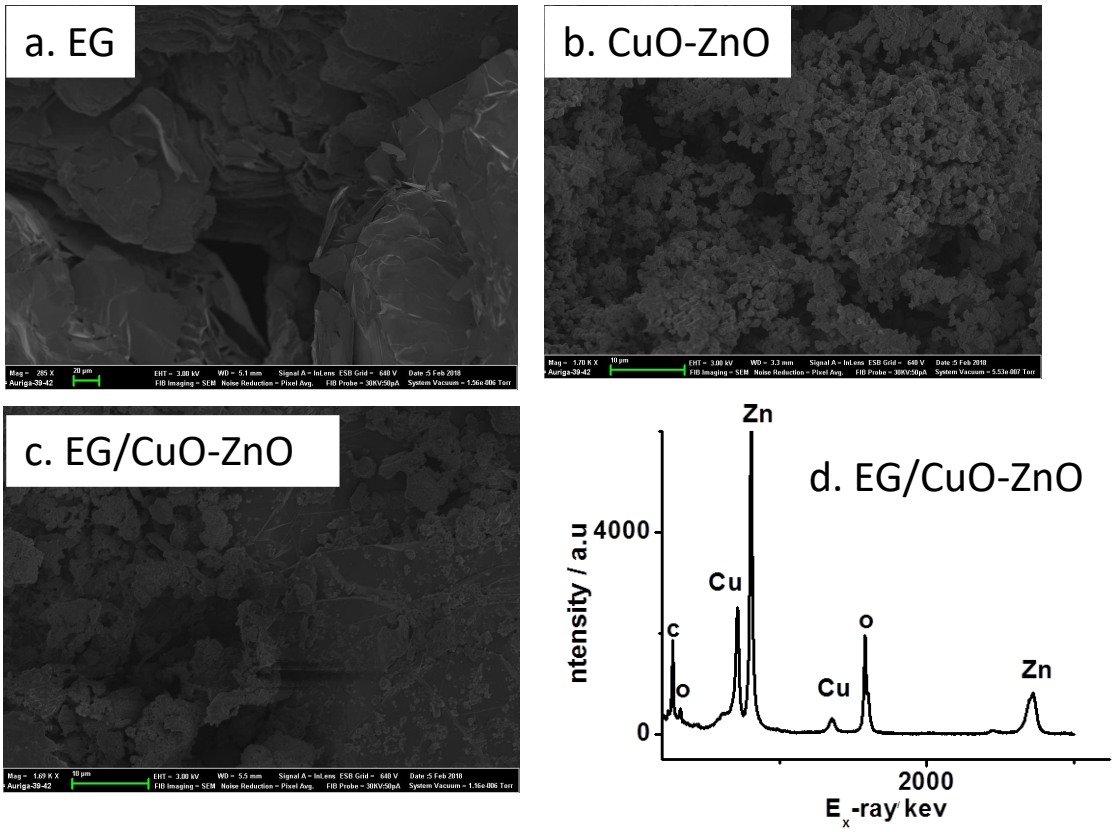

Figure 1. SEM Image of (a) EG, (b) CuO-ZnO, (c) EG/CuO-ZnO and (d) EDX

3.2 Thermogravimetric Analysis (TGA)

Fig. 2 below details TGA analysis of the utilized nanocomposites in this study. As can be seen from the Figure, the measurement was carried out at temperature ranges of 100 to 1000^{o}C. Fig. 2b shows the pure EG with a slight weight loss (%) from 100-200^{o} C. This is attributed to the retained moisture and some volatile organic compounds from the synthesized EG which were being evaporated as the temperature increased. Thereafter, a constant curve can be seen between 200^{o} C and 700^{o} C. Eventually, pyrolysis occurred from 700^{o} C to 800^{o} C, and the associated weight-loss is assigned to the decomposition of EG. The curve for CuO-ZnO is shown in Fig. 2a. Insignificant weight-loss can be seen at the temperature ranges of 100-580^{o} C indicating minimal dehydration of the sample. Nonetheless, a considerable pyrolysis took place above 580^{o} C, and a complete decomposition of CuO-ZnO nanocomposite took place at 800^{o} C. In Fig. 2c, a constant curve can be seen from the start-up temperature to 300^{o} C. This signifies that the sample neither went through moisture loss nor weight loss within lower temperature exposure. At about 350^{o} C, a weight gain occurs up to 800^{o} C. Significantly, decomposition of EG/CuO-ZnO occurred at 900^{o} C. Relatively, it can be seen that the thermal stability of CuO-ZnO/EG is less than those of the EG and CuO-ZnO on their stand-alone utilization. As observed from previous studies, this observation is a definite likelihood of the material possessing better degradation efficiency [17].

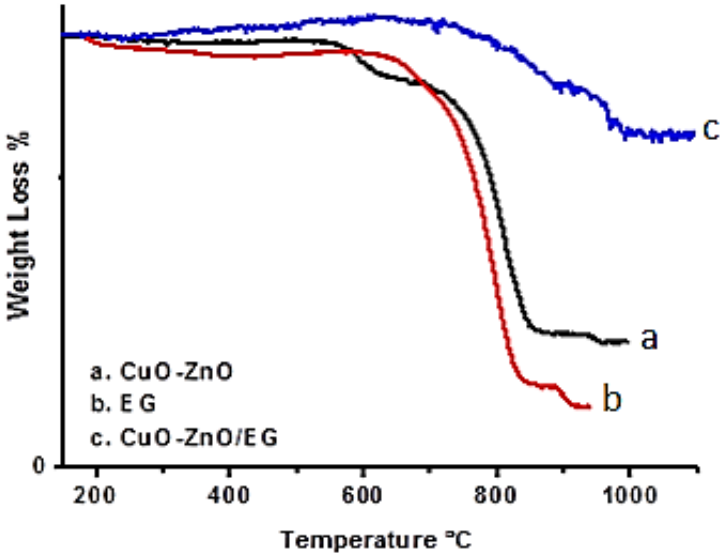

Figure 2. TGA Plots of (a) EG, (b) EG-ZnO and (c) EG/CuO-ZnO

3.3 XRD Analysis

Fig. 3 shows the XRD patterns of the EG, CuO-ZnO and EG/CuO-ZnO nanocomposites. The XRD patterns were matched with the standard JCPDS card numbers 89-0511 (ZnO) and 01-1117 (CuO) representing hexagonal ZnO and cubic CuO phases. EG exhibited a strong diffraction peak at 26.4˚ attributable to reflection plane (210) of graphite lattices in EG. With reference to the previous studies, the typical peaks of CuO-ZnO are all within the range of individual CuO and ZnO nanoparticles [18]. Furthermore, sharp and high-intensity peaks can be observed at 33 and 36˚ for CuO-ZnO. Thus, the EG/CuO-ZnO spectrum shows peaks of both EG and CuO-ZnO. Clearly, the incorporation of EG into CuO-ZnO led to peaks broadening, and thus a smaller crystallite size [18]. Smaller crystallite sizes of EG-based photoanodes is a good indication of an efficient photoelectrochemical degradation process [9, 19].

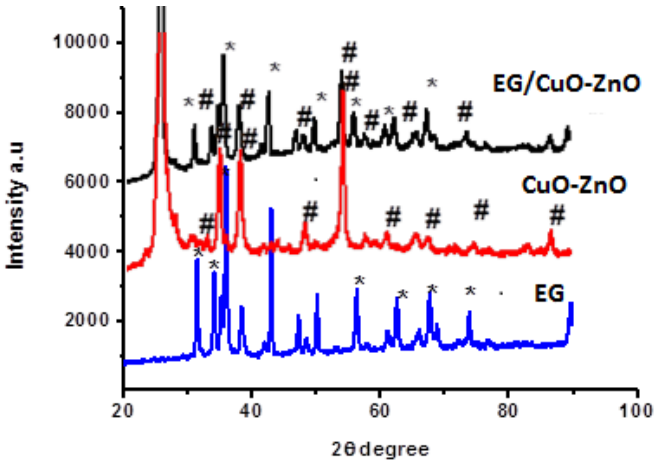

Figure 3. XRD Patterns of EG, CuO-ZnO and EG/CuO-ZnO

3.4 UV-Vis Analysis

The UV-Vis measurements were used to study the optical properties of the nanocomposites. The analysis was recorded from 200-800 nm. As can be seen in Fig. 4, particularly within the range between 400-600 nm, EG incorporation to the CuO-ZnO increases absorbance. In fact, EG/CuO-ZnO (Fig 4a) showed a higher visible light absorption compared to the pure EG and CuO-ZnO. This occurrence can be assigned to the surface plasmon resonance band effects of CuO nanoparticles that act as a photosensitizer and the presence of EG which serve as a photosensitizer for the visible light absorption.

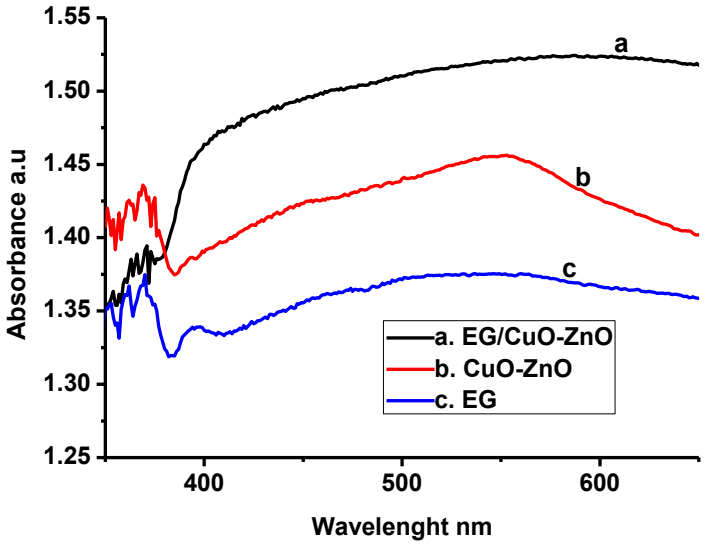

Figure 4. UV-Vis Absorbance Spectra of (a) EG/CuO-ZnO, (b) CuO-ZnO and (c) EG

3.5 BET Analysis

Table 1. BET data of EG, CuO-ZnO and EG/CuO-ZnO

Sample	BET surface area/m^2 g^{-1}	Pore volume/cm^3 g^{-1}
EG	88.45	0. 03885
CuO-ZnO	23.86	0.06723
EG/CuO-ZnO	26.96	0. 07765

BET analysis was performed with the utilization of Micromeritics Trista II surface area and porosity analyser. The results of this analysis are shown in Table 1 and they consist of BET surface area and pore volume of EG, CuO-ZnO and EG/CuO-ZnO nanocomposites. Ideally, EG surface area was found to be much higher than that of CuO-ZnO. On the other hand, the pore volume of EG was

almost half to that of CuO-ZnO as can be seen in Table 1. Significantly, when both materials are combined, both the surface area and the pore volume of EG/CuO-ZnO were higher than those of CuO-ZnO. There exist a direct relationship between a large surface area of a photoanode and improved photoelectrochemical degradation efficiency [16]. Hence, the EG/CuO-ZnO photoanode is expected to exhibit comparatively higher photoelectrochemical degradation efficiency.

3.6 Electrochemical Study

The electrochemical study on EG and EG/CuO-ZnO electrodes were performed in 2 mM [Fe (CN) 6]$^{-3/-4}$ (in 0.1 M KNO_3) solution at the scan rate of 20 mV S^{-1}. As can be seen in Fig. 5a, the EG electrode exhibited a lower current in comparison with the EG/CuO-ZnO electrode shown in Fig. 5b. Furthermore, the reduction potential of EG/CuO-ZnO (0.8 V) is higher than that of EG (0.6 V). The EG/CuO-ZnO electrode, therefore, shows faster electron transmission kinetics than the EG electrode. This enhancement is due to the increase in surface area [20] as a result of the nanocomposites added to the EG.

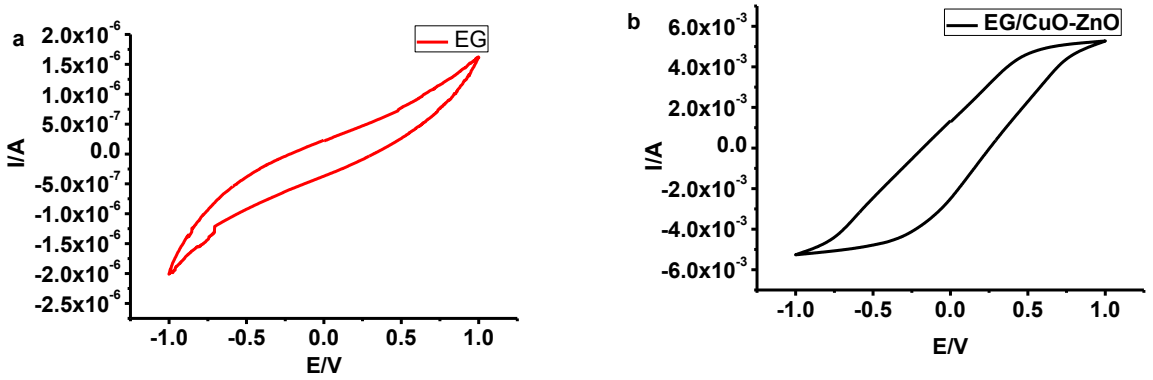

Figure 5. Cyclic Voltammograms of EG and EG/CuO-ZnO in 2 mM $K_3Fe(CN)_6$.

Fig 6 shows the electrochemical impedance spectroscopy (EIS) measurements of EG and EG/CuO-ZnO which were carried out from the open circuit potential (0.0 Volt) and the frequency range of 0.1-100 kΩ. As can be seen from the Nyquist diagram shown in Fig 6 (i), the semicircle for EG/CuO-ZnO became more compressed than that of EG, particularly at higher frequency range. This occurrence could be an indication of faster charge transfer resistance between EG/CuO-ZnO fabricated electrode and the electrolyte [21]. To prove this observation in the Nyquist diagrams, an electrical equivalent circuit (EEC) was fitted on both EG and EG/CuO-ZnO. The utilized EEC is shown in front of the Nyquist diagrams shown in Fig 6 (i). The resultant charge transfer resistance (Rct) values were 0.230kΩ and 0.431kΩ for EG/CuO-ZnO and EG respectively. The suppression of Rct observed when EG is incorporated to CuO-ZnO shows that the arc radius of EG/CuO-ZnO is smaller than that of EG and that is ideal for the efficient photoelectrochemical process [22]. Furthermore, the bode modulus plots of EG/CuO-ZnO and EG which are shown in Fig 6 (ii) and Fig 6 (iii) respectively, and the phase

plots of EG/CuO-ZnO and EG also shown in Fig. 6 (iv) and Fig 6(v) respectively, corroborate the Nyquist diagrams as the impedance and phase angles are low at low-frequency range for EG/CuO-ZnO.

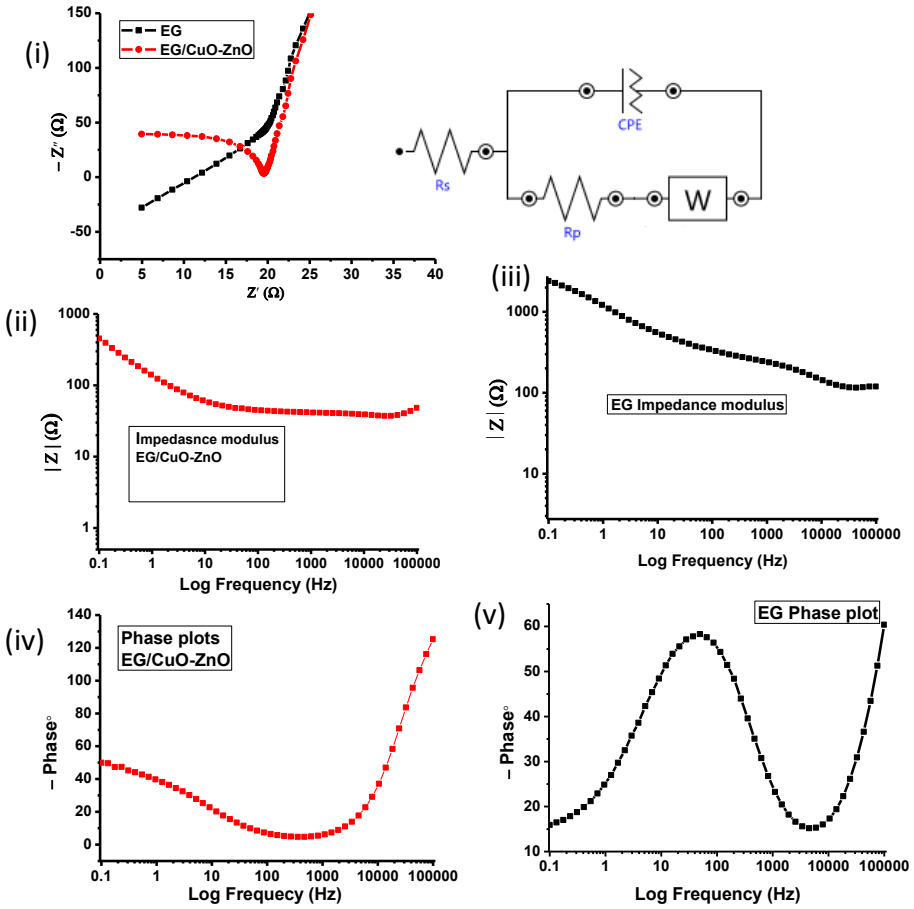

Figure 6. (i) Nyquist diagrams of EG and EG/CuO-ZnO (ii) EG/CuO-ZnO impedance modulus (iii) EG impedance modulus, (iv) EG/CuO-ZnO phase Plot and (v) EG phase Plot

3.7 Photoelectrochemical degradation study of 4-Nitrophenol

The EG/CuO-ZnO electrode was used for the degradation of 4-Nitrophenol under photoelectrochemical measurements (Fig 7b). The degradation extent was monitored by means of a visible spectrophotometer within optimum settings of pH 7 and 2.5 V. As can be seen in Fig. 7b, a gradual reduction in the intensities of the peaks occurs, and that indicates the removal of the 4-Nitrophenol from the solution as time goes on. This observation furthermore confirms the EG/CuO-ZnO fabricated electrode as a suitable photoanode for effective photoelectrochemical degradation of 4-Nitrophenol in aqueous solution.

Fig. 8a reveals EG to degrade 4-Nitrophenol to minimal efficiency, while EG/CuO-ZnO electrode showed higher degradation efficiency. In fact, about 85 % degradation of the pollutant was observed in a progression time of 280 min by the EG/CuO-ZnO electrode. The degradation efficiency

was observed to occur in the following order: EG < CuO-ZnO < EG/CuO-ZnO. The degradation experiment was also performed on three techniques: photoelectrochemical, photolysis and electrochemical oxidation. These methods in questions were engaged for the relative overview on the efficiency of dye degradation. As it can be seen in Fig. 8, the photoelectrochemical method shows a faster degradation when compared to photolysis and electrochemical oxidation. Similar observation has also been made by other authors [23]. The main distinction between these methods is that the electrochemical oxidation was performed without light, the photolysis process was carried out in the absence of a potential while the photoelectrochemical method was carried out in the presence of both the potential and light.

The inefficiency of the dye degradation through photolysis can be attributed to the rapid recombination rate of the photogenerated electrons with the holes [24]. This is particularly more pronounced when the fabricated electrode is not composed of an EG as electrons trap nanocomposite. On the other hand, the occurrence of electrochemical oxidation reaction depends on the adsorption and interaction of $^{\bullet}OH$ groups with the pollutant on the electrode's surface resulting in the degradation of the pollutant. However, the $^{\bullet}OH$ groups, upon adsorption, react with each other and produce oxygen molecules in the system instead of oxidizing the pollutant [25]. These oxygen molecules inhibit the direct interaction between the $^{\bullet}OH$ group and the pollutant causing a significant reduction in the number of adsorbed pollutant molecules on the electrode's surface [25]. It is this low pollutant adsorption phenomenon that is responsible for the comparatively low degradation efficiency of the electrochemical oxidation process. With regards to photocatalysis, the generated electrons play the role of converting oxygen molecules to superoxide radicals ($^{\bullet}O_2$) [26]. Therefore, there is no oxygen side reaction in the photocatalytic degradation process that inhibits its efficiency. Also, the CuO-ZnO present in the composite possesses the ability to produce $^{\bullet}OH$ when it is excited with photons of appropriate energy thereby improving the degradation efficiency. As a result, the photoelectrochemical degradation technique, which consists of both the electrochemical oxidation and photocatalysis, degraded the dye with the highest efficiency when compared to the individual photolysis and electrochemical oxidation processes.

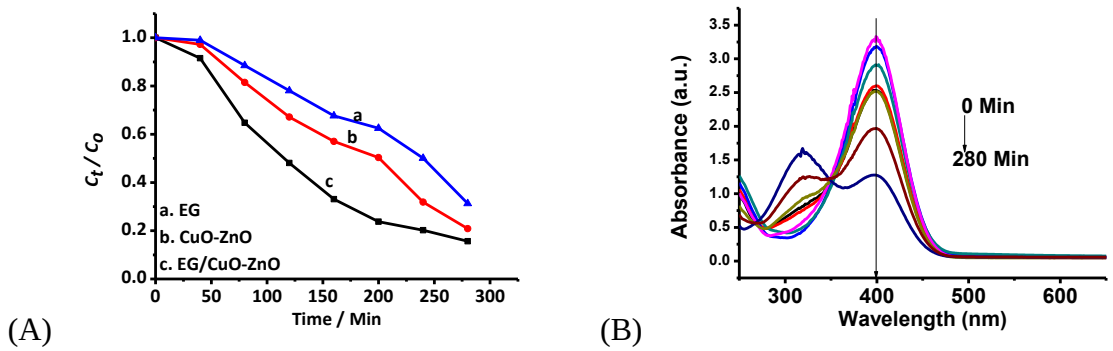

Figure 7. 4-nitrophenol degradation profiles of (A) EG, CuO-ZnO and EG/CuO-ZnO (B) EG/CuO-ZnO

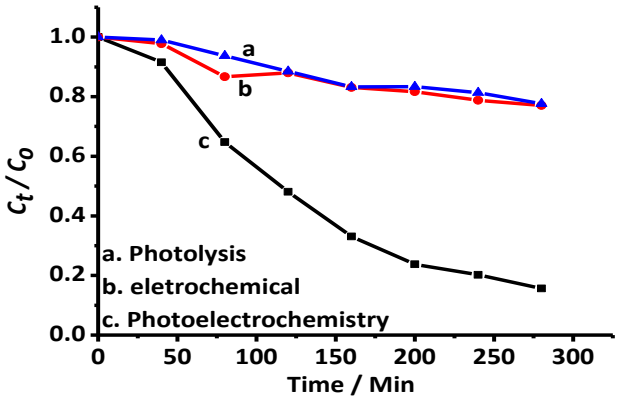

Figure 8. 4-nitrophenol degradation profiles of (A) EG, (B) CuO-ZnO and (C) EG/CuO-ZnO

It was deemed necessary to compare the effectiveness of the EG/CuO-ZnO electrode with other published results involving the degradation of 4-nitrophenol. The result of this analysis is presented in Table 2. It is clear, according to Table 2, that EG/CuO-ZnO electrode shows a higher degradation efficiency compared to other is compared to the other catalysts used for the degradation of 4-nitrophenol. The EG/CuO-ZnO can, therefore, be considered as an effective catalyst for the degradation of 4-nitrophenol.

Table 2. Comparison of the effectiveness of the EG/CuO-ZnO electrode with other published results

Name of Catayst	Name of Pollutant	Degradation Efficiency %	References
RKJ300	4-nitrophenol	80	[27]
C, N-TiO_2	4-nitrophenol	65	[28]
G/TiO_2	4-nitrophenol	59.5	[29]
Expanded graphite-TiO2	4-nitrophenol	62	[30]
Fe–TiO2	4-nitrophenol	67.5	[31]
CuO-ZnO/EG	4-Nitrophenol	85	[present work]

In order to determine how reliable the EG/CuO-ZnO electrode is for multiple usages in the degradation of 4-Nitrophenol in aqueous solution, five consecutive cycles of photoelectrochemical degradation were run from 0 to 280 min. As shown in Fig. 9, a good photoelectrochemical re-usage can be observed, and that shows a quasi-nil existence of secondary pollution which is avoided in degradation. Therefore, the fabricated EG/CuO-ZnO utilized along with photoelectrochemical degradation technique in this study is successful in the degradation of 4-Nitrophenol from the aqueous solution.

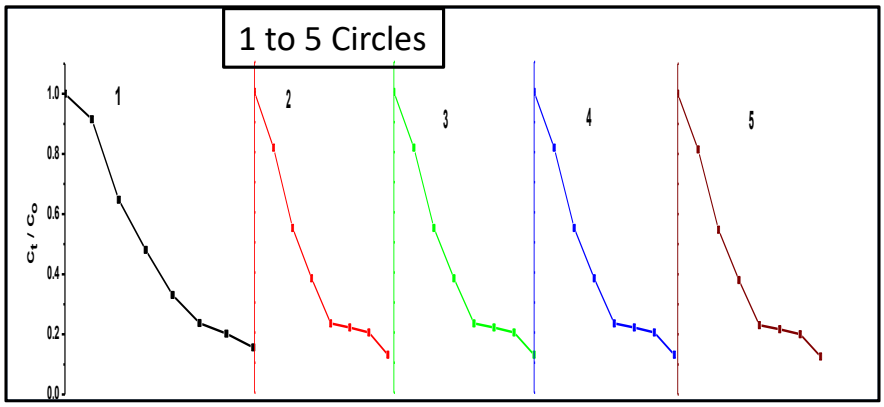

Figure 9. Five cycle degradation test of the EG/CuO-ZnO electrode for the photoelectrochemical degradation of 4-Nitrophenol

4. CONCLUSION

This study achieved synthesis, fabrication and characterization of EG, CuO-ZnO and EG/CuO-ZnO nanocomposites for the degradation 4-Nitrophenol from the aqueous solution. The following conclusions were drawn up:

- XRD and EDX analyses revealed the successful synthesis of the EG/CuO-ZnO nanocomposites while the SEM images showed the CuO-ZnO nanoparticles to be evenly dispersed on the surface of the synthesized EG.
- The EG/CuO-ZnO exhibited improved visible light absorption as compared to the pure EG and CuO-ZnO, and that resulted in a higher photoelectrochemical degradation efficiency.
- The photoelectrochemical technique was observed to be more efficient than photolysis and photochemical oxidation methods on their single utilization.
- The photoelectrochemical degradation method achieved about 82 % degradation efficiency within 280 min and can be recycled over a number of times without losing its efficiency.

ACKNOWLEDGEMENTS
The University of Johannesburg is acknowledged for financial support for this Research, and National Research Foundation (NRF) South Africa is gratefully acknowledged by the Authors.

References

1. G. Hurwitz, P. Pornwongthong, S. Mahendra, E.M. Hoek, Chem. *Eng. J.*, 240 (2014) 235.
2. J. Cao, B. Xu, H. Lin, B. Luo, S. Chen, *Dalton Trans.*, 41 (2012) 11482.
3. K. K. Paul, R. Ghosh, P. K. Giri, *Nanotechnology*, 27 (2016) 315703.
4. S. Li, X. Lu, Y. Xue, J. Lei, T. Zheng, C. Wang, *PLoS One*, 7 (2012) 43328.
5. S.H.S. Chan, T. Yeong Wu, J.C. Juan, C.Y.J. Teh, *Chem. Technol. Biotechnol.*, 86 (2011) 1130
6. G.R.P. Malpass, D.W. Miwa, A.C.P. Miwa, S.A.S. Machado, A.J. Motheo, *Environ. Sci. Technol.*, 41(2007) 7120.
7. A.S. Stasinakis, *GLOBAL NEST J*, 10 (2008) 376.

8. X. Zhao, Y. Zhu, *Environ. Scie & Technol.,* 40 (2006) 3367.
9. C. Yang, X. Cao, S. Wang, L. Zhang, F. Xiao, X. Su, J. Wang, *Ceram. INT.,* 41 (2015) 1749.
10. P. Sathishkumar, R. Sweena, J.J. Wu, S. Anandan, *Chem. Eng. J.,* 171 (2011) 136.
11. O.M. Ama, O.A. Arotiba, *J. Electroanal .Chem.,* 803 (2017) 157.
12. R.M. Asmussen, M. Tian, A. Chen, *Environ. Scie & Technol.,* 43 (2009) 5100.
13. J. Ahmad, K. Majid, *Adv Compos Hybrid Mater,* 1 (2018) 1.
14. A.D. Manasrah, I.W. Almanassra, N.N. Marei, U.A. Al-Mubaiyedh, T. Laoui, M.A. Atieh, *RSC Advances,* 8 (2018) 1791.
15. Y.T. Chung, M.M. Ba-Abbad, A.W. Mohammad, A. Benamor, *Desalin Water Treat.,* 57 (2016)7801.
16. M. Mansournia, L. Ghaderi, J. *Alloys Compd.,* 691 (2017) 171.
17 A.D. Manasrah, I.W. Almanassra, N.N. Marei, U.A. Al-Mubaiyedh, T. Laoui, M. Atieh, *RSC Advances,* 8 (2018) 1791.
18. W. He, L. Zhu, H. Chen, H. Nan, W. Li, H. Liu, Y. Wang, *Appl. Surf. Sci.,* 279 (2013) 416.
19. O.M. Ama, N. Kumar, F.V. Adams, S.S. Ray, *Electrocatalysis,* 1 (2018) 1.
20. EH Umukoro, M.G. Peleyeju, J.C. Ngila, O.A. Arotiba, *RSC Advances,* 6 (2016) 52868.
21. Y. Zhou, W. Fang, Y. Deng, I. Pan, B. Shen, H. li, J. Zhang, *Rsc advances,* 7 (2017), 55927.
22. C. Wang, F. Wang, M. Xu, C. Zhu, W. Fang, Y. Wei, J. *Electroanal. Chem,* 759 (2015) 158.
23. A Socha, E. Sochocka, R. Podsiadły, J. Sokołowska, *Color Technol.,* 122 (2006) 207.
24. C.A.P. Arellano, S.S. Martínez, *Sol. Energ. Mat. Sol. C.,* 94 (2010) 327.
25. L. Lin, Y. Chai, B. Zhao, W. Wei, D. He, B. He, Q. Tang, *OJIC.,* 3 (2013)14.
26. W.W. Anku, S.K. Shukla, P.P Govender, *J. Inorg. Organomet. P.,* 28 (2018)1540.
27. A. Ghosh, M. Khurana, A. Chauhan, M.Takeo, A.K. Chakraborti, R.K. Jain, *Environ. Sci. Technol.,* 44 (2010)1069.
28. A.O. Oluwatomiwa , T. Yu, X. Cai, Y. Jiang, G. Peng, X. Cheng, R. Li, Y. Qin, S. Lin, *Front Chem.,* 6 (2018) 192.
29. X. Liu, L. Zhao, H. Lai, S. Li, Z. Yi. *J Chem. Technol. Biot.,* 92 (2017) 2417.
30. B. Ntsendwana, S. Sampath, B.B. Mamba, O.A. Arotiba, *Photoch. Photobio Sci.,* 12(2013)1091.
31. B. Zhao, G. Mele, I. Pio, J. Li, L. Palmisano, G. Vasapollo, *J. Hazard. Mater.,* 176 (2010) 569